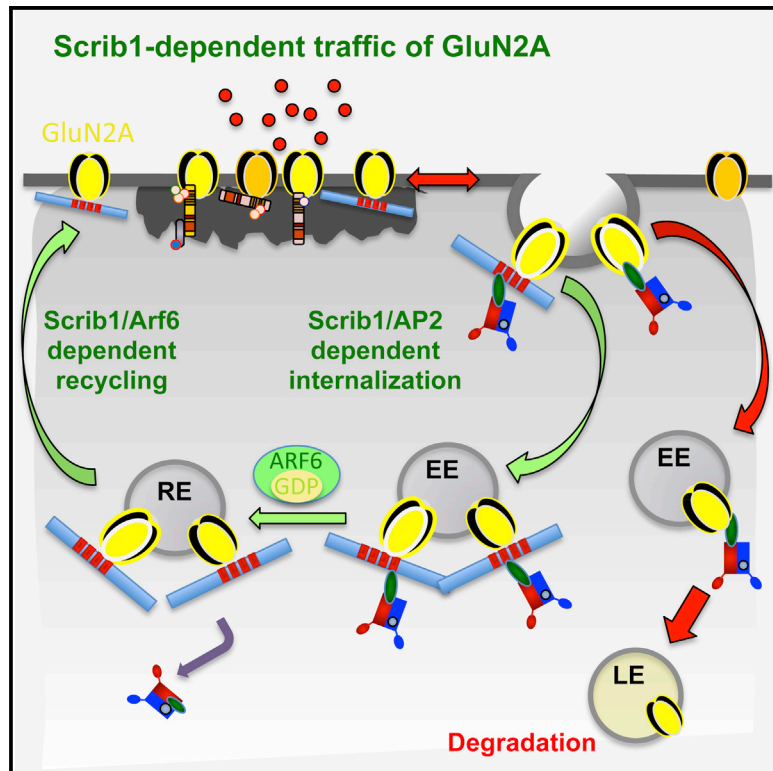# Cell Reports

# Scribble1/AP2 Complex Coordinates NMDA Receptor Endocytic Recycling

## Graphical Abstract



## Authors

Nicolas H. Piguel, Sabine Fievre, ..., Claudia Racca, Nathalie Sans

## Correspondence

nathalie.sans@inserm.fr

## In Brief

Scribble1 (Scrib1) plays a major role in apico-basal and planar cell polarity in epithelial cells and was recently implicated in synaptic transmission and plasticity. Here, Piguel et al. report that Scrib1 is a key mediator of the endocytic sorting of NMDARs through its selective interactions with the AP2 complex. This Scrib1-dependent mechanism is likely to be involved in the regulation of synapse function in numerous physiological processes and pathological states that involve NMDARs.

## Highlights

Scrib1 is regulated in an activity-dependent manner

Scrib1 drives the recycling of GluN2A subunits

AP2 interacts with Scrib1 YxxR motif to control NMDAR postendocytic traffic

Scrib1 is required for NMDAR maintenance at CA3-CA1 synapses

CellPress

# Article

# Scribble1/AP2 Complex Coordinates NMDA Receptor Endocytic Recycling

Nicolas H. Piguel,[1,2] Sabine Fievre,[3,4] Jean-Michel Blanc,[1,5,6] Mario Carta,[3,4] Maïté M. Moreau,[1,2] Enora Moutin,[7,8,9] Vera L. Pinheiro,[1,2] Chantal Medina,[1,2] Jerome Ezan,[1,2] Léa Lasvaux,[1,2] François Loll,[1,2] Christelle M. Durand,[1,2] Kai Chang,[10] Ronald S. Petralia,[10,11] Robert J. Wenthold,[10,14] F. Anne Stephenson,[12] Laurent Vuillard,[6] Hervé Darbon,[5] Julie Perroy,[7,8,9] Christophe Mulle,[3,4] Mireille Montcouquiol,[1,2] Claudia Racca,[13] and Nathalie Sans[1,2,*]

[1]Physiopathologie de la Plasticité Neuronale, Neurocentre Magendie, INSERM, U862, 33000 Bordeaux, France
[2]Neurocentre Magendie, University of Bordeaux, U862, 33000 Bordeaux, France
[3]Institut Interdisciplinaire de Neurosciences, University of Bordeaux, UMR 5297, 33000 Bordeaux, France
[4]Institut Interdisciplinaire de Neurosciences, CNRS, UMR 5297, 33000 Bordeaux, France
[5]Architecture et Fonction des Macromolecules Biologiques, UMR 7257, Campus de Luminy, CNRS/Aix-Marseille Universite, 13288 Marseille, France
[6]BioXtal Structural Biology Unit, Campus de Luminy, 13288 Marseille, France
[7]UMR-5203, Institut de Génomique Fonctionnelle, CNRS, 34000 Montpellier, France
[8]INSERM, U661, 34000 Montpellier, France
[9]Universités de Montpellier 1 and 2, UMR 5203, 34000 Montpellier, France
[10]Laboratory of Neurochemistry, National Institute on Deafness and Other Communication Disorders, National Institutes of Health, Bethesda, MD 20892, USA
[11]Advanced Imaging Core of NIDCD, National Institutes of Health, Bethesda, MD 20892, USA
[12]University College London School of Pharmacy, London WC1N 1AX, UK
[13]Institute of Neuroscience, Newcastle University, Newcastle upon Tyne NE2 4HH, UK
[14]Deceased
*Correspondence: nathalie.sans@inserm.fr
http://dx.doi.org/10.1016/j.celrep.2014.09.017

## SUMMARY

The appropriate trafficking of glutamate receptors to synapses is crucial for basic synaptic function and synaptic plasticity. It is now accepted that NMDA receptors (NMDARs) internalize and are recycled at the plasma membrane but also exchange between synaptic and extrasynaptic pools; these NMDAR properties are also key to governing synaptic plasticity. Scribble1 is a large PDZ protein required for synaptogenesis and synaptic plasticity. Herein, we show that the level of Scribble1 is regulated in an activity-dependent manner and that Scribble1 controls the number of NMDARs at the plasma membrane. Notably, Scribble1 prevents GluN2A subunits from undergoing lysosomal trafficking and degradation by increasing their recycling to the plasma membrane following NMDAR activation. Finally, we show that a specific YxxR motif on Scribble1 controls these mechanisms through a direct interaction with AP2. Altogether, our findings define a molecular mechanism to control the levels of synaptic NMDARs via Scribble1 complex signaling.

## INTRODUCTION

NMDA receptors (NMDARs) are widely distributed in the brain, where they play a key role in synapse development, synaptic transmission, and plasticity (Traynelis et al., 2010). GluN2A and GluN2B are differentially localized in neurons, and GluN2A is reportedly more stable and synaptic than GluN2B, which is more mobile and preferentially, but not exclusively, found at extrasynaptic sites (Lau and Zukin, 2007; Wenthold et al., 2003; Yashiro and Philpot, 2008). The polarized trafficking process of GluN2A and GluN2B has been intensively studied, but the pathways controlling NMDAR trafficking processes remain poorly understood (Lau and Zukin, 2007; Wenthold et al., 2003; Yashiro and Philpot, 2008).

PSD-95/discs-large/ZO-1 (PDZ) domain-containing proteins were identified as the major synaptic scaffolding proteins anchoring the NMDAR at glutamatergic synapses (Elias and Nicoll, 2007; Sheng and Hoogenraad, 2007). The initial PDZ-based interaction studies with membrane-associated guanylate kinases (MAGUKs) led to the identification of many PDZ proteins and their roles in glutamate receptor (GluR) anchoring and trafficking. It is now believed that NMDARs are dynamically associated with PDZ proteins that play various and specific roles in their trafficking to and/or from synapses, either by direct sorting, exocytosis from internal compartments, internalization, recycling, or lateral movements (Elias and Nicoll, 2007; Groc et al., 2009; Lau and Zukin, 2007; Sheng and Hoogenraad, 2007; Wenthold et al., 2003; Yashiro and Philpot, 2008). Synaptic NMDARs appear to be exchanged with extrasynaptic receptors and to be recycled through clathrin-dependent endocytosis, but NMDAR subunits seem to behave differently (Groc et al., 2006; Lavezzari et al., 2004; Montgomery et al., 2005; Pérez-Otaño et al., 2006; Prybylowski et al., 2005; Scott et al., 2004). GluN2A subunits are preferentially trafficked through the late endosome

pathway for degradation after internalization; GluN2B subunits are constitutively recycled (Lau and Zukin, 2007; Lavezzari et al., 2004). Moreover, during activation, the presence of GluN2A at synapses is favored and GluN2B is degraded (Barria and Malinow, 2002; Jurd et al., 2008). Several proteins, such as PDZ proteins (i.e., MAGUKs; Chung et al., 2004; Howard et al., 2010; Losi et al., 2003; Mauceri et al., 2007; Sans et al., 2003), soluble NSF attachment protein receptor (SNARE)-related proteins (Lau et al., 2010; Sans et al., 2003; Suh et al., 2010), or kinases (Prybylowski et al., 2005; Sanz-Clemente et al., 2010, 2013) can specifically affect membrane NMDAR subunit levels and the GluN2A/GluN2B ratio. This complex trafficking of NMDARs participates in the fine-tuning of excitatory synapses and in some types of long-term potentiation and long-term depression (Yashiro and Philpot, 2008).

Scribble1 (Scrib1) is a highly conserved protein that contains 16 leucine-rich repeat domains, two LAP domains, and four PDZ domains. Recently, we showed that Scrib1 participates in the development of hippocampal neurons and that a *circletail* mutant form impacts not only learning and memory but also social behavior (Moreau et al., 2010). Here, we decipher an original molecular and functional relationship between Scrib1 and NMDAR subunits that identifies Scrib1 as a key regulator of synaptic fine-tuning of excitatory synapses.

## RESULTS

### Scribble1 Interacts with the PDZ Binding Domain of the GluN2A and GluN2B Subunits

We performed a yeast two-hybrid screen with the PDZ domains of Scrib1 to probe a mouse P10 brain yeast two-hybrid library as described previously (Yi et al., 2007). We isolated a clone containing the sequence of GluN2A. In a two-hybrid screen with the C termini of the GluN2A subunit as bait, we isolated a clone that encoded the entire PDZ domain region of Scrib1. Consequently, we used the PDZ domains of Scrib1 as prey and found that pGBKT7-GluN2A or -GluN2B chimeras interacted strongly with these PDZ domains, whereas removal of the last seven amino acids of GluN2A or GluN2B (including the PDZ binding domain or PDZ-BD) prevented the interaction (Figure 1A). In human embryonic kidney 293 (HEK293) cells cotransfected with GFP-Scrib1, GFP-Scrib1ΔPDZ, and Tac-GluN2A or Tac-GluN2B chimeric transmembrane proteins, we were able to coimmunoprecipitate GFP-Scrib1. This interaction was lost upon deletion of the PDZ domains of Scrib1 (GFP-Scrib1ΔPDZ), indicating that Scrib1 interacts with NMDARs through its PDZ domain (Figure 1B). In pull-down experiments, the PDZ domains 2 and 3 of Scrib1 were able to bind independently to GluN2A and GluN2B fusion proteins (data not shown). Isothermal titration calorimetry (ITC) experiments revealed that both the GluN2A and GluN2B peptides bound to PDZ2 with a $K_D$ of approximately 60 μM for GluN2A and 48 μM for GluN2B and to PDZ3 with a $K_D$ of 11.6 μM for GluN2A and 12.3 μM for GluN2B. The binding of PDZ4 was weaker, with a $K_D$ over 150 μM, whereas no binding was observed with PDZ1 (Figures 1C and 1D; Table S1). We also tested the PDZ binding domain mutant peptides (GluN2A$^{S1462A}$ and GluN2B$^{S1480A}$) and observed no binding (Figures 1E and 1F; Table S1). Taken together, these data demonstrate that

Scrib1 PDZ2 and PDZ3 interact specifically with the PDZ-BD of the GluN2A and GluN2B subunits.

### The Spatio temporal Localization of Scribble1 Matches that of NMDARs

We examined the temporal expression and localization of Scrib1 in the rat brain. As illustrated in Figure 1G, Scrib1 expression level decreased from postnatal day 0 (P0) to adult with a persistent expression at P120. Other related proteins, such as densin-180 and Erbin, displayed different developmental profiles (Figure 1G). The early and strong expression of Scrib1 matches that of GluN2B and overlaps with GluN2A in later stages (starting at P9), which is consistent with an interaction of Scrib1 with the GluN subunits. The interaction of Scrib1 with the GluN1, GluN2A, and GluN2B subunits, but not with the GABA$_A$ receptor β3 subunit, was confirmed by coimmunoprecipitation (coIP) (Figure 1H).

Using postembedding immunogold electron microscopy, we showed that Scrib1 is localized with NMDARs postsynaptically at excitatory synapses in the stratum radiatum of the CA1 region of the hippocampus (Figures 1I–1K and S1A–S1G; Scrib1: 5 nm gold particles and GluN1: 15 nm gold particles). We also found Scrib1 associated with NMDARs in intracellular vesicles or organelles in the dendritic spine (Figures S1H and S1I). These localizations are consistent with our in vitro data and coIP experiments.

### Scrib1 and GluN2A Levels Increase at Active Synapses

To investigate whether the levels of Scrib1 were relevant for function, we analyzed whether they were regulated by synaptic activity. We used the Na$^+$ channel blocker tetrodotoxin to block synaptic activity or the GABA$_A$ receptor antagonist bicuculline to increase excitatory activity by blocking inhibitory GABAergic transmission in cultured neurons. Enriched synaptosome preparations showed that Scrib1 levels mirrored GluN2A profile of expression and accumulated in active synaptosome fractions (Figures 2A and 2B). These data suggest that levels of Scrib1 and GluN2A-containing NMDARs are correlated and that Scrib1 participates in NMDAR regulation at the membrane to modify synaptic strength.

To investigate whether Scrib1 and NMDAR levels were also regulated by activity in vivo, we examined whether exposure of adult rats to a new enriched environment modified Scrib1 and NMDAR levels. Rats were subjected to an enriched open field for 10 min and left undisturbed in their home cages for 1 hr before collecting the hippocampus (enriched open field [EOF] animals), whereas control group rats were placed in their home cages until tissue collection (control; Figure 2C). Results showed that Scrib1 levels increased significantly in hippocampi of EOF rats compared to the control group (p < 0.01; Figure 2D). This upregulation of Scrib1 in the hippocampus of EOF rats was accompanied by a significant increase of GluN2A and a slight but significant reduction of GluN2B in the synaptosomal fraction (p < 0.05; Figure 2E). In hippocampal membrane fraction, Scrib1 coimmunoprecipitated GluN2A around 30% more in EOF condition than in basal conditions whereas the levels of GluN2B were not significantly different (Figures 2F and 2G). These results show that exposure to a new environment leads to a major increase in
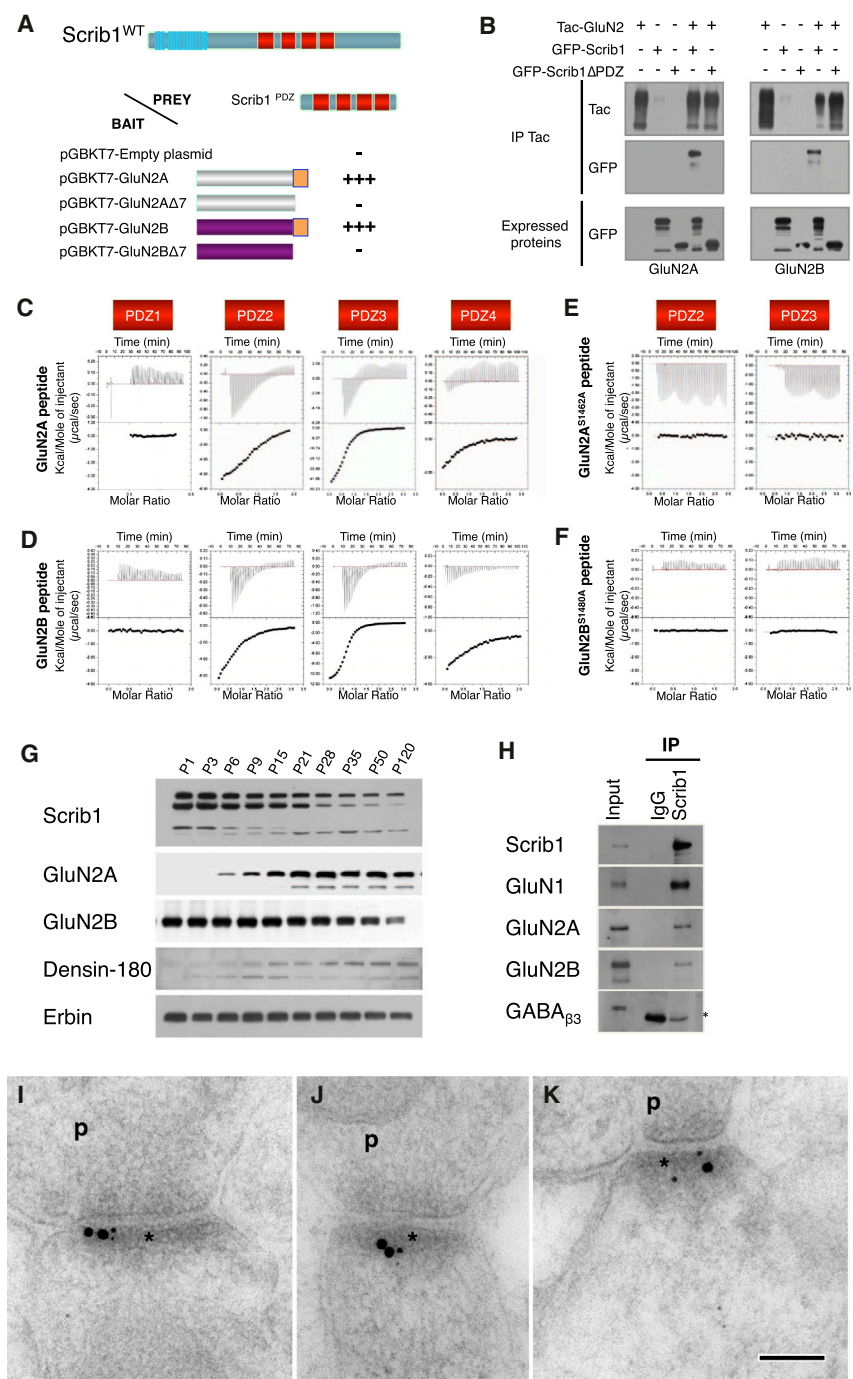
## Figure 1. Scrib1 Interacts and Colocalizes with GluN2 Subunits

(A) Directed yeast two-hybrid assays with GluN2A, GluN2B, and Scrib1 constructs. Schematic domain structures of GluN2 C-terminal used as bait. Scrib1 binds the PDZ binding domain of GluN2A and GluN2B. For the same concentration and same dilution, >40 colonies grew on 4DO plates for 2A and 2B baits whereas none for Δ7 constructs after 4 days at 30°C.

(B) Lysates from HEK293 cells transfected with GFP-Scrib1 or GFP-Scrib1$^{\Delta PDZ}$ and Tac-GluN2A or Tac-GluN2B and immunoprecipitated with Tac antibodies. The precipitates were immunoblotted with anti-GFP or anti-Tac. GFP-Scrib1 coimmunoprecipitates with Tac-GluN2A and TacGluN2B.

(C–F) Calorimetric titrations of Scrib1 PDZs interaction with GluN2A (C), GluN2B (D), GluN2A$^{S1462A}$ (E), and GluN2B$^{S1480A}$ (F) peptides. Top: ITC heat variation after each ligand; the first peak corresponds to a small amount of injected ligand. Bottom: the corrected heat developed per mole of ligand. This curve allows the determination of the dissociation constant using the theory of Wiseman isotherm.

(G) Developmental protein expression pattern of Scrib1 and the GluN2A and GluN2B from P1 to P120 in rat hippocampus homogenates (30 μg protein per lane) analyzed by SDS-PAGE and immunoblotted with the antibodies described in the Supplemental Experimental Procedures. At all ages, the samples were analyzed with the different antibodies obtained from the same preparation of hippocampus. Representative results, n = 3 experiments.

(H) Endogenous coIP of Scrib1, GluN2A, and GluN2B from the hippocampus. The 100,000 × g detergent supernatants were immunoprecipitated with Scrib1 antibodies. The precipitates show positive immunoblotting for GluN2A and GluN2B subunits, but not β3-containing GABA$_A$ receptor (star, bands in IP correspond to immunoglobulin G [IgG]).

(I–K) Immunogold localization of Scrib1 (5 nm) and its colocalization with GluN1 (15 nm) in hippocampal CA1 stratum radiatum synapses. Note the double labeling in PSD. Asterisk, postsynaptic density; p, presynaptic terminal. The scale bar represents 100 nm.
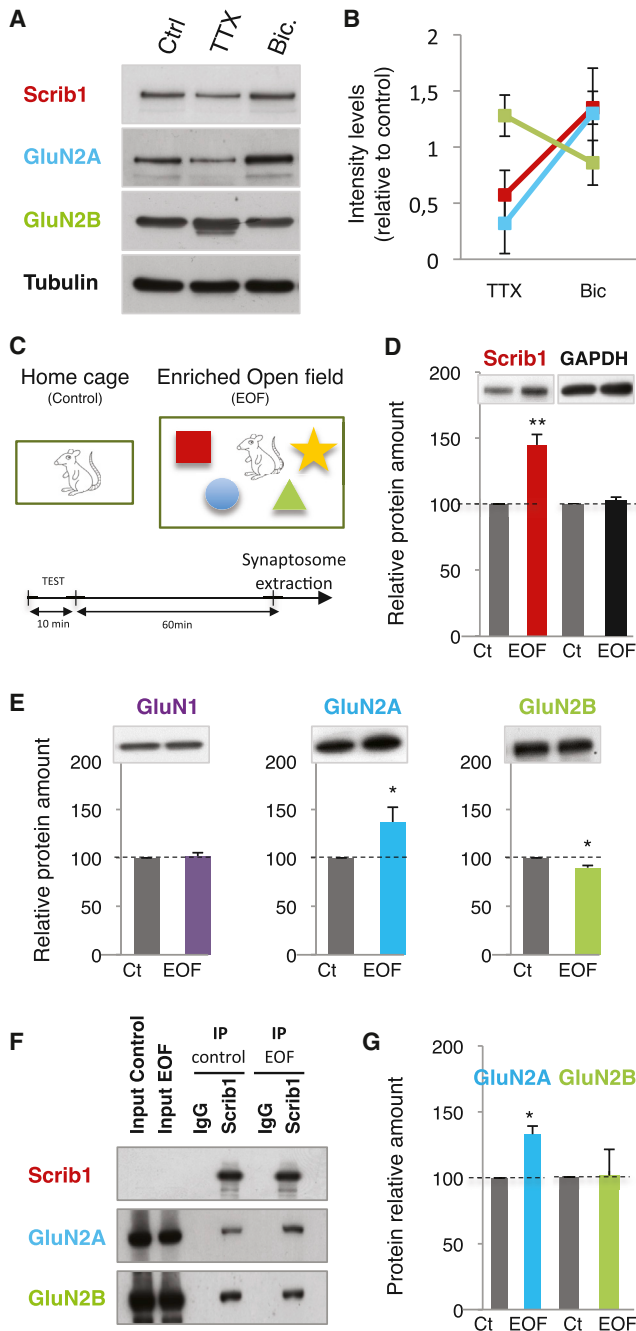
commercially available N-terminal GluN2B from Alomone Labs. Number of puncta and global intensity of native GluN2A or GluN2B increased in the presence of GFP-Scrib1 protein (GluN2A puncta: Ctrl: 23.33 ± 0.75 versus Scrib1: 27.75 ± 0.99, p < 0.05; intensity: 74.67 ± 2.55 versus 90.23 ± 3.96, p < 0.01; GluN2B puncta: 20.97 ± 0.64 versus 25.22 ± 1.26, p < 0.01; intensity: 96.57 ± 3.85 versus 113.73 ± 5.25, p < 0.05; Figures 3A, 3B, 3D, and 3E), whereas surface staining for both subunits was not different in the presence of a mutated form of Scrib1 missing the two PDZ domains implicated in the interaction with NMDAR (GluN2A puncta: Ctrl: 23.33 ± 0.75 versus GFP-Scrib1$^{\Delta PDZ2-3}$: 21.51 ± 0.61, p = 0.065; intensity: 74.67 ± 2.55 versus 78.47 ± 3.25, p = 0.36; GluN2B puncta: 20.97 ± 0.64 puncta versus

Scrib1 expression and modifies the amount of Scrib1-NMDAR subunit content in the hippocampus.

## Scrib1 Levels Regulate Native NMDA Surface Receptors in Hippocampal Neurons

To determine the consequences of the levels of Scrib1 on the surface expression of native GluN2A and GluN2B receptors, we used loss- and gain-of-function approaches. We used the N-terminal antibodies developed against GluN2A (Groc et al., 2006) and the

**Figure 2. Expression of Scrib1 and GluN Proteins Is Regulated by Activity in the Hippocampus**

(A) Immunoblot analysis of Scrib1, GluN2A, GluN2B, and tubulin in synaptic fractions isolated from cortical neurons treated 48 hr with control solution, TTX (2 μM), or bicuculline (Bic.) (40 μM).

(B) Quantitative analysis of the abundance of Scrib1 (red), GluN2A (blue), and GluN2B (green) in synaptic fractions treated with TTX or bicuculline of the band intensities 48 hr after drug treatment and normalized to the control values from the untreated control neuron synaptic fraction. Note that abscissa values reflect drug treatments. All data are presented as mean ± SEM (n = 3 experiments). Error bars are all ± SEM.

(C) Experimental design protocol of the hippocampal synaptosome extraction after new environment stimulation in an enriched open field (EOF).

20.35 ± 0.52, p = 0.45; intensity: 96.57 ± 3.85 versus 97.2 ± 3.86, p = 0.48; Figures 3A, 3C, 3D, and 3F). On the other hand, down-regulation of Scrib1 led to a decrease of the density of surface staining of native GluN2A or native GluN2B (GluN2A: small hairpin control [shCtrl]: 23.69 ± 0.67 versus shScrib1: 16.82 ± 0.83, p < 0.001; GluN2B: 20.03 ± 0.85 versus 16.23 ± 0.49, p < 0.01; Figures 3G, 3H, 3J, and 3K). The total intensity for GluN2A in dendrites measured as the ratio of the surface-staining intensity per unit area was also decreased (69.99 ± 2.81 versus 58.05 ± 2.9, p < 0.05; Figures 3G and 3I). Surprisingly, a similar quantification revealed no change in this ratio for GluN2B (92.96 ± 4.48 versus 104.02 ± 4.32, p = 0.08; Figures 3J and 3L). We found the same trend with transfected myc-GluN2A or myc-GluN2B (Figure S2). We were able to rescue the sh-induced phenotype using an sh-resistant form of Scrib1, but not with the mutated form of Scrib1 missing the two PDZ domains (GluN2A/shScrib1 puncta: rescue by Scrib1: 24.42 ± 0.78 versus no rescue by GFP-Scrib1$^{\Delta PDZ2-3}$: 16.11 ± 0.46, p < 0.001; intensity: 74.99 ± 3.66 versus 57.09 ± 3.32, p < 0.01; GluN2B/shScrib1 puncta: rescue: 21.89 ± 0.9 versus no rescue: 16.09 ± 0.53, p < 0.01; intensity: 94.62 ± 4.47 versus 104.64 ± 5.43, p = 0.17; Figures 3G–3I and 3J–3L). Scrib1 overexpression or downregulation had no impact on native α1-containing GABA$_A$ receptors (Figures 3M and 3N) or on the number of synapses (Figures 3O and 3P). Altogether, our results show that Scrib1 levels affect NMDA surface receptors via PDZ2 and PDZ3 interaction with GluN2 because the Scrib1 mutated form missing these two specific domains has no effect on NMDAR trafficking.

## Differential Regulation of Native NMDA Surface Receptors after D-Serine Stimulation prior to NMDA/D-Serine Activation
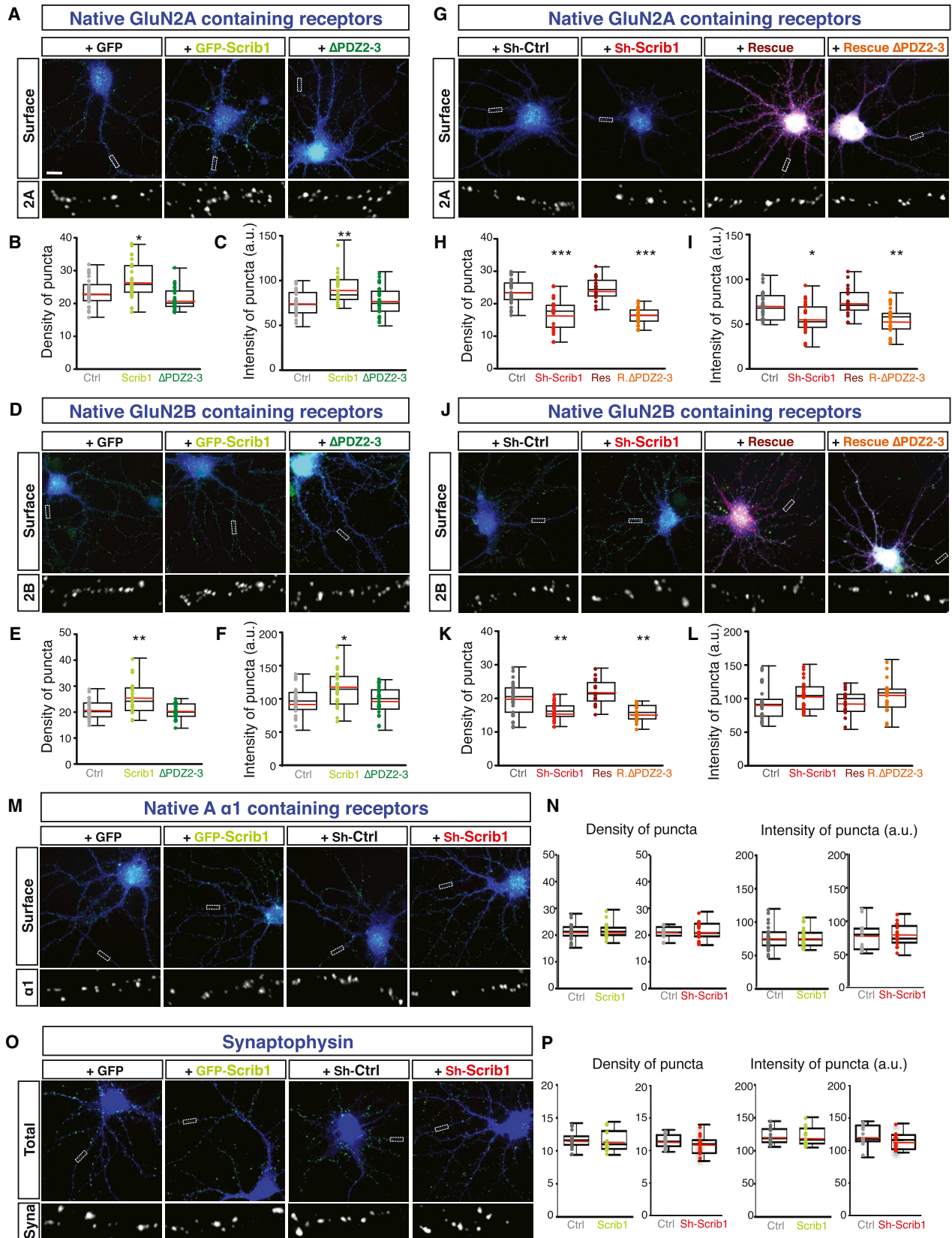
To investigate whether a stimulation of the receptors could differently modify the surface expression of NMDAR depending on Scrib1 levels, we compared basal conditions to D-serine stimulation prior to NMDA/D-serine activation, thus "priming" the NMDAR (Nong et al., 2003). After stimulation, surface staining of native GluN2A increased with increased Scrib1 levels and decreased with decreased Scrib1 levels as shown previously without stimulation (GluN2A puncta: Ctrl: 24.97 ± 0.56 versus Scrib1: 29.28 ± 0.84 puncta, p < 0.001; shCtrl: 24.36 ± 0.34 versus shScrib1: 20.92 ± 0.38, p < 0.001; Figures S3A and S3B). Total intensity varied in the same manner (Figures S3A and S3B). However, after stimulation, surface staining of native GluN2B

(D) Quantitation of Scrib1 and GAPDH levels in hippocampus extracts by western blot.

(E) Western blot of GluN1, GluN2A, and GluN2B protein in P2 subcellular fractionation of rat hippocampus lysates. Error bars are all ± SEM.

(F) Endogenous coIP of GluN2A and GluN2B with Scrib1 from the hippocampus of control or EOF rats. The 100,000 × g detergent supernatants were immunoprecipitated with anti-Scrib1. Ten microliters of bound immunoprecipitate fractions were separated by SDS-PAGE; immunoblotted; and incubated with Scrib1, GluN2A, or GluN2B antibodies. Percentage of immunostaining in the bound fraction is shown in (G).

(G) Quantitation of the IP bands normalized to control (100% = control gray histograms). Levels were measured using the ChemiDoc MP imager system. There is a significant difference in GluN2A-bound fraction to Scrib1 in the EOF compared to control condition. Error bars are all ± SEM.

**A** Native GluN2A containing receptors

+ GFP | + GFP-Scrib1 | + ΔPDZ2-3

**B** Density of puncta — Ctrl, Scrib1, ΔPDZ2-3 *

**C** Intensity of puncta (a.u.) — Ctrl, Scrib1, ΔPDZ2-3 **

**D** Native GluN2B containing receptors

+ GFP | + GFP-Scrib1 | + ΔPDZ2-3

**E** Density of puncta — Ctrl, Scrib1, ΔPDZ2-3 **

**F** Intensity of puncta (a.u.) — Ctrl, Scrib1, ΔPDZ2-3 *

**G** Native GluN2A containing receptors

+ Sh-Ctrl | + Sh-Scrib1 | + Rescue | + Rescue ΔPDZ2-3

**H** Density of puncta — Ctrl, Sh-Scrib1 ***, Res, R.ΔPDZ2-3 ***

**I** Intensity of puncta (a.u.) — Ctrl, Sh-Scrib1 *, Res, R-ΔPDZ2-3 **

**J** Native GluN2B containing receptors

+ Sh-Ctrl | + Sh-Scrib1 | + Rescue | + Rescue ΔPDZ2-3

**K** Density of puncta — Ctrl, Sh-Scrib1 **, Res, R.ΔPDZ2-3 **

**L** Intensity of puncta (a.u.) — Ctrl, Sh-Scrib1, Res, R.ΔPDZ2-3

**M** Native A α1 containing receptors

+ GFP | + GFP-Scrib1 | + Sh-Ctrl | + Sh-Scrib1

**N** Density of puncta — Ctrl, Scrib1 / Ctrl, Sh-Scrib1 ; Intensity of puncta (a.u.) — Ctrl, Scrib1 / Ctrl, Sh-Scrib1

**O** Synaptophysin

+ GFP | + GFP-Scrib1 | + Sh-Ctrl | + Sh-Scrib1

**P** Density of puncta — Ctrl, Scrib1 / Ctrl, Sh-Scrib1 ; Intensity of puncta (a.u.) — Ctrl, Scrib1 / Ctrl, Sh-Scrib1

*(legend on next page)*

decreased with increased Scrib1 levels and increased with decreased Scrib1 levels (GluN2B puncta: Ctrl: 19.00 ± 0.52 versus Scrib1: 16.58 ± 0.64, p < 0.01; shCtrl: 19.05 ± 0.47 versus shScrib1: 22.69 ± 0.4, p < 0.001; Figures S3C and S3D). The total intensity varied in the same manner (Figures S3C and S3D). Altogether, these data suggest that Scrib1 regulates the pool of surface GluN2A and GluN2B dynamically, depending on neuronal activity context, and the stimulation or not of NMDARs affect differently the pool of surface GluN2A and GluN2B.

## Scrib1 Interacts with Tac-GluN2A and Tac-GluN2B Chimeras at the Plasma Membrane and in Endosomes of COS-7 Cells

To investigate the involvement of Scrib1 in NMDAR internalization and recycling, we carried out experiments in COS-7 cells with NMDAR subunit chimeras. In these cells, Scrib1 was redistributed and colocalized with GluN2 chimeras at the plasma membrane and in vesicle-like clusters (Figures S4A and S4B) and the removal of the PDZ-BD of the chimeras (Tac-GluN2AΔ7 or Tac-GluN2BΔ7) abolished this redistribution (Figures S4C and S4D).

The localization of the GluN2 chimeras-Scrib1 complex in intracellular clusters suggests two nonmutually exclusive possibilities: (1) these clusters are involved in the sorting of GluN2 chimeras from the Golgi complex to the plasma membrane and/or (2) Scrib1 is associated with internalized receptors. First, surface staining was performed to validate that some of the Scrib1 puncta colocalized with surface Tac-GluN2A and Tac-GluN2B chimeras (data not shown). After 15 min of internalization, we observed a complete colocalization of Scrib1/internalized GluN2 chimeras with Rab5a (Figures S4E and S4F). After 30 min of internalization, the majority of Tac-GluN2A was colocalized with CD63 in late endosomes and lysosomes and only 20% was associated with Rab11 in recycling endosomes (Figures S4G and S4H) as previously published (Lavezzari et al., 2004). In the presence of Scrib1, we observed a shift in the localization of the GluN2A chimeras, with 40% of the GluN2A chimeras found in Rab11-positive recycling endosomes (Figures S4G, S4H, S4K, and S4L). Scrib1 expression slightly increased the colocalization of GluN2B with Rab11 in recycling endosomes (Figures S4I and S4J) and decreased the colocalization with CD63 (Figures S4M and S4N). Scrib1 promotes GluN2A chimera

recycling (Figures S4O and S4P) and to a lesser extent GluN2B chimera recycling (Figures S4Q and S4R). These results show that Scrib1 participates in Tac-GluN2A and Tac-GluN2B internalization and favors the recycling pathway in COS-7.

## Scrib1 Levels Differentially Modulate myc-GluN2A and myc-GluN2B Internalization in Hippocampal Neurons

Next, we wanted to determine whether Scrib1 affected specifically internalization or recycling of GluN2A and/or GluN2B subunits in hippocampal neurons. First, we examined whether an upregulation or downregulation of Scrib1 could modulate internalization of GluN2 subunits (Figure 4A). Because these experiments require a large amount of antibodies, we used surface-expressed receptors. We also compared basal conditions to D-serine stimulation after priming the NMDAR for endocytosis, as before. Increasing Scrib1 levels did not change the internalized/surface ratio of myc-GluN2A or myc-GluN2B (Ps > 0.1; Figures 4B, 4C, 4F, and 4H). The activation of NMDARs significantly reduced the surface expression of myc-GluN2A independently of Scrib1 levels (stimulus effect: p < 0.001; treatment effect: p = 0.10; Figures 4B and 4F). Decrease of Scrib1 levels had the opposite effect on the internalization of both subunits (Figures 4D, 4E, 4G, and 4I). In basal conditions, a decrease of Scrib1 levels increased the internalization/surface ratio of GluN2A, whereas this ratio was decreased for GluN2B (p < 0.001; Figures 4D, 4E, 4G, and 4I). The activation of NMDARs in neurons with decreased Scrib1 levels abolished the effect seen in basal conditions for GluN2B (p > 0.3; Figures 4D, 4E, 4G, and 4I). Using an sh-resistant form of Scrib1, we could rescue the sh-induced phenotype for GluN2A (Figures 4J and 4K) or GluN2B (Figures 4L and 4M) in basal conditions. Together, these data show that the upregulation of Scrib1 does not change the internalized/surface ratio of either GluN2A or GluN2B in basal or activated conditions. On the other hand, the downregulation of Scrib1 has a differential effect on the internalized/surface ratio of GluN2A and GluN2B.

## Scrib1 Facilitates myc-GluN2A Recycling in Hippocampal Neurons

We tested whether Scrib1 levels modulated NMDAR subunit recycling after internalization in neurons (Figure 5A). Recycling experiments under basal conditions showed that increased Scrib1

**Figure 3. Modification of Scrib1 Levels Affects Surface Expression of Endogenous GluN2A and GluN2B-Containing Receptors**

(A–C) Surface staining of endogenous GluN2A-containing NMDAR with overexpression of GFP-control, GFP-Scrib1, or GFP-Scrib1ΔPDZ2-3 in primary hippocampal neuron culture (A) and box-and-whisker plots indicate the median value (black line) and mean value (red line), the 25th–75th (box), and the 10th–90th (whiskers); open circles represent individual values for GluN2A puncta number (B) or intensity (C).

(D–F) Surface staining of endogenous GluN2B-containing NMDAR with overexpression of GFP-control, GFP-Scrib1, or GFP-Scrib1ΔPDZ2-3 in primary hippocampal neuron culture (D) and box-and-whisker plots; open circles represent individual values for GluN2B puncta number (E) or intensity (F).

(G–I) Surface staining of endogenous GluN2A-containing NMDAR with overexpression of sh-control, sh-Scrib1, or rescue with Scrib1 or Scrib1ΔPDZ2-3 in primary hippocampal neuron culture (G) and box-and-whisker; open circles represent individual values for GluN2A puncta number (H) or intensity (I).

(J–L) Surface staining of endogenous GluN2B-containing NMDAR with overexpression of sh-control, sh-Scrib1, or rescue with Scrib1 or Scrib1ΔPDZ2-3 in primary hippocampal neuron culture (J) and box-and-whisker plots; open circles represent individual values for GluN2B puncta number (K) or intensity (L).

Data were compared using Kruskal-Wallis one way with Dunn's multiple comparison. a.u., arbitrary units (n = 20–30 neurons).

(M and N) Surface staining of endogenous α1-containing GABAAR with overexpression of GFP-control or GFP-Scrib1 and sh-control or sh-Scrib1 in primary hippocampal neuron culture (M) and box-and-whisker plots; open circles represent individual values puncta number (left) or intensity (right; N).

(O and P) Surface staining of endogenous synaptophysin with overexpression of GFP-control or GFP-Scrib1 and sh-control or sh-Scrib1 in primary hippocampal neuron culture (O) and box-and-whisker plots; open circles represent individual values puncta number (left) or intensity (right; P).

Data were compared using t test (n = 15–26 neurons). The scale bar represents 10 μm.
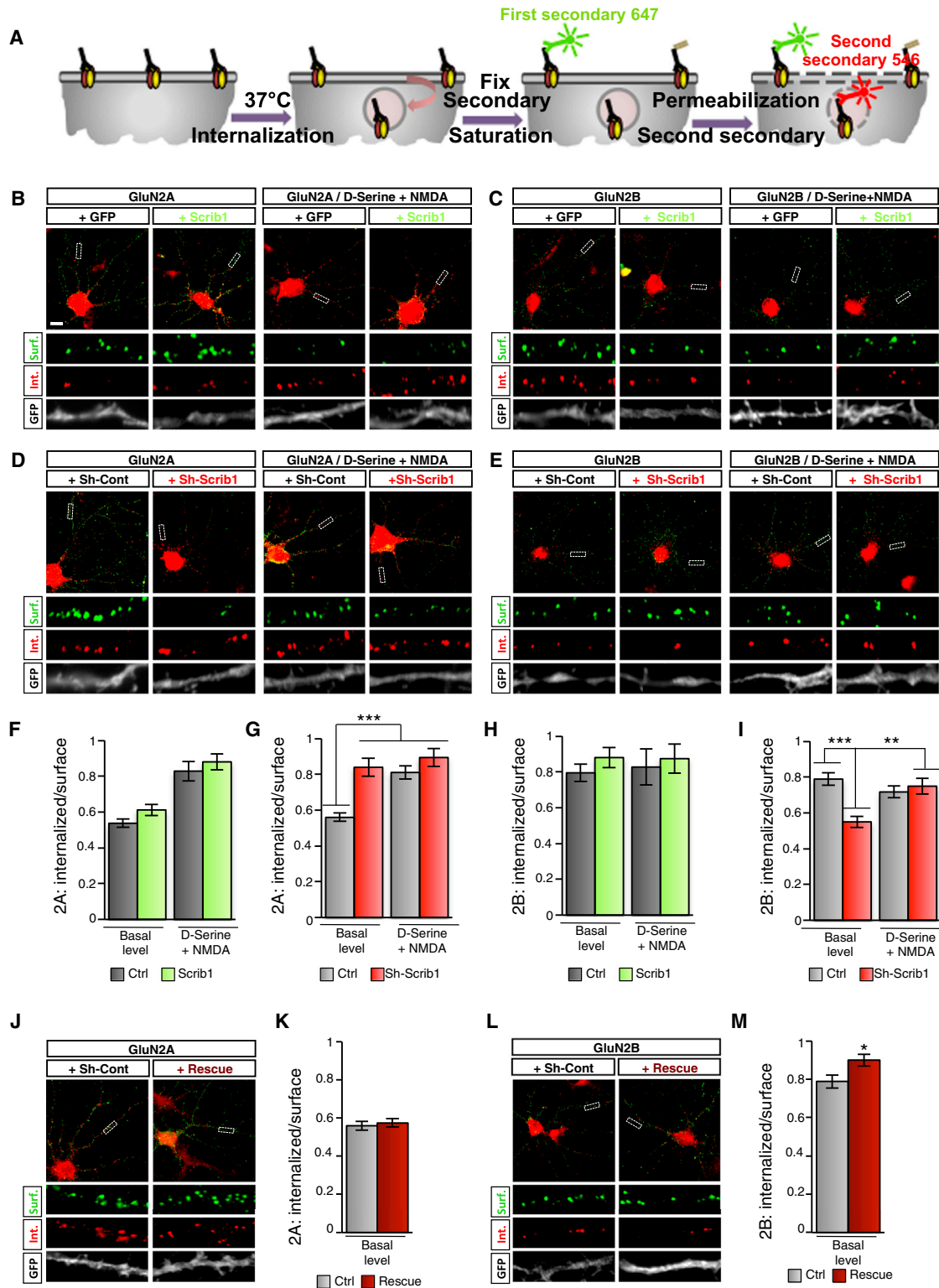
**Figure 4. The Loss of Scrib1 Stabilizes GluN2B and Increases GluN2A Internalization**

(A) Timeline of the endocytosis experiments.

(B and C) Internalization of GluN2A-containing NMDARs (B) and GluN2B-containing NMDARs (C) with or without stimulation, respectively. Primary hippocampal neuron cultures were transfected with myc-GluN2A (B) or myc-GluN2B (C) and GFP-control or GFP-Scrib1 at 14 or 15 DIV.

*(legend continued on next page)*

levels specifically increased the recycling of internalized myc-GluN2A back to the plasma membrane, which is otherwise degraded (p < 0.001; Figures 5B and 5F), but had no effect on GluN2B (p = 0.79; Figures 5C and 5H) or GABA$_A$ receptor β3 subunit (p = 0.99; data not shown). Additional activation of NMDARs further increased recycling of the internalized GluN2A back to the plasma membrane in the presence of overexpressed Scrib1 (p < 0.01; Figures 5B and 5F) and significantly decreased the recycling of GluN2B, independently of Scrib1 overexpression (p < 0.001; Figures 5C and 5H). Thus, NMDARs activation influenced differently the recycling traffic of GluN2A and GluN2B in the presence of Scrib1 through a specific GluN2A recycling increase whereas GluN2B recycling appeared insensitive to Scrib1 increased levels.

Loss-of-function experiments were done to evaluate the impact of decreased levels of Scrib1 expression. Under basal conditions, decreased Scrib1 levels did not affect the recycling rate of GluN2A at the membrane (p = 0.70; Figures 5D and 5G). NMDAR activation slightly increased the recycling of GluN2A, which was abolished in the absence of Scrib1 (p < 0.05; Figures 5D and 5G). Under basal conditions, downregulation of Scrib1 levels significantly decreased GluN2B recycling at the membrane (p < 0.001; Figures 5E and 5I). Notably, NMDAR activation changed the ratio of recycled/internalized GluN2B; here, downregulation of Scrib1 increased the recycling of GluN2B compared to control shRNA (p < 0.001). To further decipher the Scrib1-dependent trafficking pathway, we performed endosomal staining in neurons transfected with GFP-Rab11 and GFP-CD63, 30 min after internalization of myc-GluNs in the presence of hemagglutinin (HA)-Scrib1 (Figure S5) or mCherry-pSuper-Scrib1 (Figure S6). As expected, we observed a stronger colocalization of GluNs with Rab11 than with CD63 for all the conditions showing an increasing recycling. On the contrary, a decrease in recycling was always associated with a stronger colocalization with CD63 at the expense of Rab11 (Figures S5 and S6). In conclusion, GluN2A and GluN2B behave differently in response to the expression level of Scrib1: Scrib1 upregulation affects the recycling of GluN2A more than that of GluN2B, whereas Scrib1 downregulation blocks GluN2A recycling, with opposite effects on GluN2B recycling depending on the activation state of the neuron.

We wanted to study the role of ARF6 in the regulation of NMDAR by Scrib1, as it is a known regulator of other transmembrane receptor (Lahuna et al., 2005). Interestingly, ARF6 increased GluN2A recycling and ARF6$^{T27N}$ (a dominant-negative form) inhibited Scrib1-dependent effect on recycling (Figures 5J

and 5K). Expression of a catalytically inactive form of ARF6 guanine nucleotide exchange factor EFA6 (EFA6-E242K), known to regulate constitutive endosomal recycling to the cell surface (Franco et al., 1999), also inhibited Scrib1-induced effect on recycling (Figures 5L and 5M). These results strongly suggest that Scrib1 regulates the recycling of GluN2A through ARF6 activation.

### The AP2 Adaptor Interacts with Scrib1 to Allow Internalization and Recycling of the NMDAR/Scrib1 Complex

Several studies have shown that PDZ proteins, such as PSD-95, stabilize NMDARs at the membrane (Groc et al., 2006; Prybylowski et al., 2005; Roche et al., 2001). In the case of GluN2B-containing NMDARs, the PDZ protein dissociates from the receptor to allow the AP2 adaptors to bind a distal YEKL motif on the GluN2B tail and to induce its internalization, which is followed by a rapid recycling of the synaptic receptor (Prybylowski et al., 2005; Scott et al., 2004). The GluN2A subunit is regulated differently (Prybylowski et al., 2005). Because Scrib1 is a PDZ protein that colocalizes with GluRs at the membrane and in endocytic vesicles, it was difficult to reconcile our data with this model. We also noticed in our electron microscopic analysis that Scrib1 was sometime present at the lateral domain of the spine (Figure 6A), where activity-dependent exocytosis and endocytosis domains have been identified (Kennedy et al., 2010). In our yeast two-hybrid screen with the PDZ-containing domains of Scrib1, we found a clone containing an ~0.7 kb insert encoding amino acids 200–429 of the open reading frame of the AP2μ subunit (NP_033809.1). Sequence analysis showed that this clone contained the C-terminal domain of AP2μ, which recognizes tyrosine-based sorting motifs, such as YxxØ (where x is a polar or charged amino acid and Ø is a hydrophobic residue; Traub, 2009). We found one putative binding site for AP2 close to the consensus sequence found in vertebrates in the Scrib1 sequence between PDZ1 and PDZ2 (Figure 6B). This sequence (YSPR) differs from the consensus sequence for AP2 binding site in substitution of the Y+3 hydrophobic residue with a charged arginine. However, it should be noted that Arg was found in this position in other proteins that bind AP2 adaptors with a strong affinity (Uekita et al., 2001). The mutation of one amino acid in this sequence prevented Scrib1 binding to AP2 both in a yeast two-hybrid assay and pull-down experiments (Figures 6C and 6D). We further validated this interaction by coimmunoprecipitation of AP2 in hippocampal lysates from P21 rats using an antibody against Scrib1 (Figure 6E). We then modeled the binding of our target sequence to AP2μ. The

---

(D and E) Internalization of GluN2A-containing NMDARs (D) and GluN2B-containing NMDARs (E) with or without stimulation, respectively. Primary hippocampal neuron cultures were transfected with myc-GluN2A (D) or myc-GluN2B (E) and sh-control or sh-Scrib1 at 14 or 15 DIV.
Surface receptor populations are labeled in green, and internalized receptor populations are in red.
(F–I) Histograms represent the means of the ratio of internalized puncta over the surface receptor puncta, corresponding, respectively, to the images in (B)–(E). (F) Data were compared using two-way ANOVA (n = 19 to 20 neurons). (G) Data were compared using two-way ANOVA and Bonferroni multiple comparison test (n = 15–20 neurons). (H) Data were compared using two-way ANOVA (n = 16–20 neurons). (I) Data were compared using two-way ANOVA and Bonferroni multiple comparison test (n = 15–17 neurons) ± SEM. Error bars are all ± SEM.
(J and K) Internalization of GluN2A-containing NMDARs with sh-control or sh-Scrib1 and shRNA-resistant HA-Scrib1 form (rescue; J) and histograms represent the means of the ratio of internalized puncta over the surface receptor puncta (K). Error bars are all ± SEM.
(L and M) Internalization of GluN2B-containing NMDARs with sh-control or sh-Scrib1 and shRNA-resistant HA-Scrib1 form (rescue; L) and histograms represent the means of the ratio of internalized puncta over the surface receptor puncta (M). Error bars are all ± SEM.
Data were compared using an unpaired t test ± SEM. The scale bar represents 10 μm.
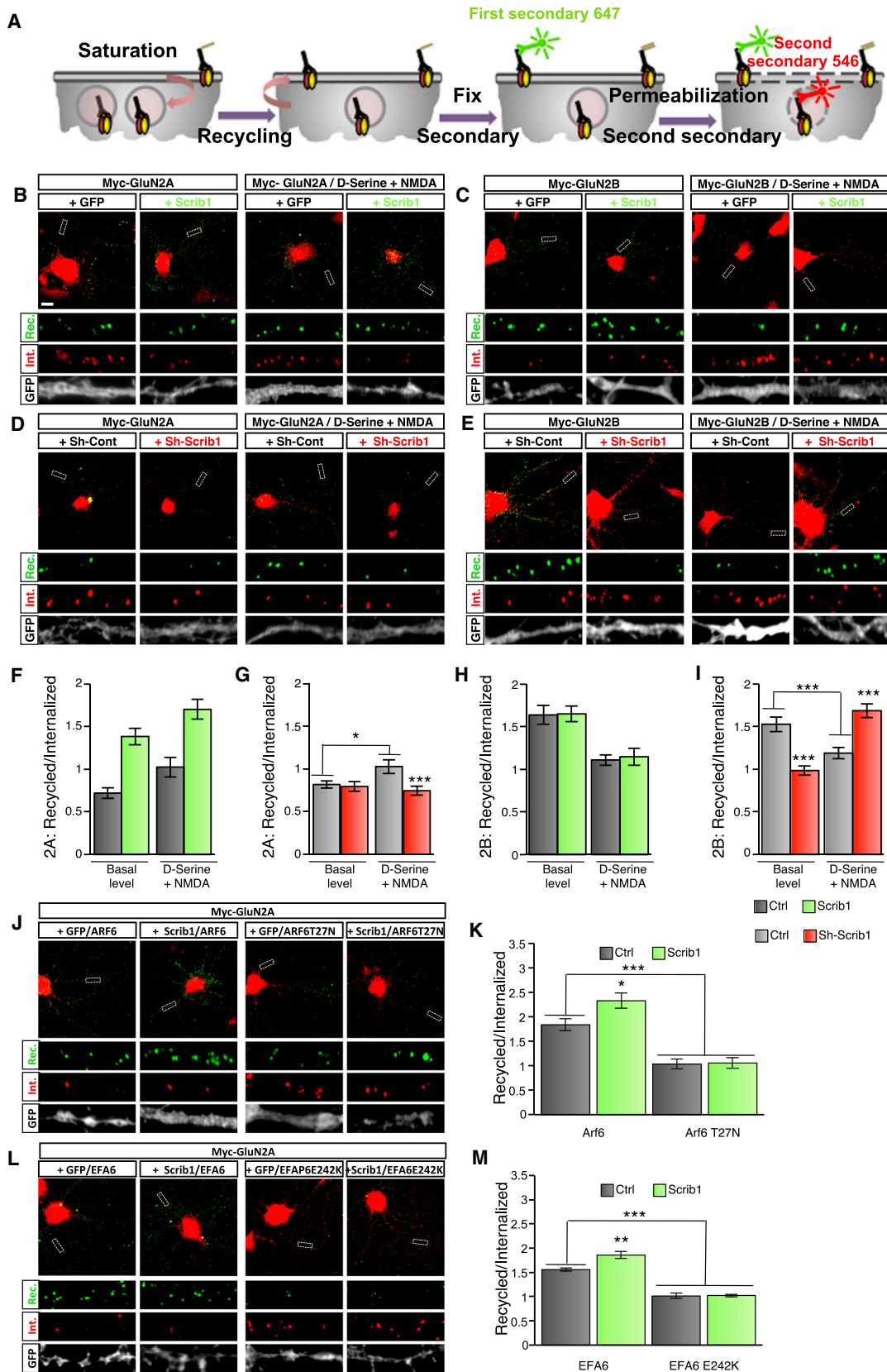
(legend on next page)

potential interacting site on Scrib1 fits in the classic binding site of AP2μ (Figures 6F–6H). In addition to the canonical Tyr834, several ionic bonds were observed (Arg839/Asp415, Glu838/Lys420, and Glu831/Arg357; Figure 6H). Notably, we identified a putative ionic bond between Glu838 and Lys420 at a position where there is typically a hydrophobic interaction, such as with residue Met204 from CTLA-4 (Follows et al., 2001). Our results suggest that the interaction of AP2 with Scrib1 uses a slightly different binding mode than the previously described associations with AP2μ. We further show that the internalizations of both GluN2A and GluN2B were reduced in the presence of a nonfunctional GFP-Scrib1$^{Y834A}$ construct in hippocampal neurons (Figure 6I). These results show that a noncanonical, vertebrate-specific, endocytic motif in Scrib1 is recognized by the AP2 adaptors. Although Scrib1 does not change the internalization rate of GluN2A or GluN2B per se, binding of the AP2 adaptors to Scrib1 plays a role in the internalization (Figures 6I–6K) and likely in the subsequent recycling of NMDARs.

### Scrib1 Regulates the Level of Synaptic NMDARs at Schaffer Collateral CA1 Pyramidal Cell Synapses

We performed single-cell electroporation of CA1 pyramidal cells in organotypic hippocampal slices with either pSUPER-shRNA-Scrib1 or pSUPER-shRNA-control. Three days after transfection, we recorded pharmacologically isolated NMDAR-mediated excitatory postsynaptic currents (EPSCs) from a transfected neuron and a neighboring nontransfected neuron in pairs (Figure 7A). Decreased levels of Scrib1 significantly reduced the amplitude of synaptic NMDAR-mediated responses compared to control (Figures 7B and 7C). The decay time of synaptic NMDAR-mediated EPSCs did not vary between the two conditions, suggesting that the acute downregulation of Scrib1 did not modify the composition of synaptic NMDARs (Figures 7B and 7C). On the other hand, in a similar experimental setting, overexpression of Scrib1 or GFP did not alter the amplitude or decay time of NMDAR-mediated EPSCs (Figure S7A). The reduction in the NMDAR-mediated EPSCs observed with the knockdown of Scrib1 could be mediated by the reduction in the number of synapses and not by a selective loss of NMDAR. To address this concern, we measured the α-amino-3-hydroxy-5-methyl-4-isoxazolepropionic acid (AMPA)/NMDA ratio in organotypic cultures. In our transfection time frame, we observed a change in the AMPA/NMDA ratio (Figure 7D). This imbalance can explain the decrease in NMDAR synaptic currents seen in Figure 7B. To further verify the selective effect on NMDAR, we measured the amplitude of pharmacologically isolated AMPA receptor (AMPAR)-mediated EPSCs and found that they were not different from controls when assessed with the paired recording experiment (Figures 7E and 7F). Our results confirm that Scrib1 downregulation affects specifically NMDAR currents with no major effect on AMPAR. The overexpression of Scrib1 did not cause any significant differences compared to control GFP (Figures S7B and S7C), suggesting that additional signals are necessary to drive the entry of GluN2A in synapses, as we have observed in Figure 2.

To confirm that the loss of Scrib1 does not alter the subunit composition of synaptic NMDARs, we tested the effect of Ro25-2981, a selective antagonist of NMDARs containing GluN2B. The effects of Ro25-2981 on the amplitude and decay time of NMDAR-mediated EPSCs in neurons transfected with pSUPER-shRNA-Scrib1 or with pSUPER-shRNA-control were not significantly different (Figure S7D) as compared to controls (Figure S7E). In conclusion, these data confirm that the loss of Scrib1 affects the levels of synaptic NMDARs in hippocampal excitatory synapses.

## DISCUSSION

Here, we identified Scrib1 as a key PDZ protein involved in the functional and spatial regulation of synaptic NMDARs. First, we found a direct physical interaction between GluN2 subunits and Scrib1. Second, we demonstrated that Scrib1 levels modulate NMDAR trafficking and recycling to the membrane through a direct interaction with the AP2 adaptor proteins and the use of regulatory proteins, such as ARF6. Third, we showed that downregulation of Scrib1 in hippocampal neurons leads to a decrease in synaptic NMDAR currents.

NMDARs play a central role in controlling synaptic transmission and plasticity. Therefore, it has been a challenge to identify the molecular mechanisms that regulate GluN2A and GluN2B synaptic expression. In our previous study, we showed that, after 5 or 6 days posttransfection, the downregulation of Scrib1 in

---

**Figure 5. Scrib1 Promotes GluN2A Recycling and Inhibits GluN2B Recycling upon Stimulation in Neuron Culture**

(A) Timeline of the recycling experiments.

(B and C) Recycling of GluN2A- (B) and GluN2B- (C) containing NMDARs with or without stimulation. Overexpression of GFP-control or GFP-Scrib1 in primary hippocampal neuron culture transfected with myc-GluN2A (B) or myc-GluN2B (C) at 14 or 15 DIV.

(D and E) Recycling of GluN2A- (D) and GluN2B- (E) containing NMDARs with or without stimulation. Overexpression of sh-control or sh-Scrib1 in primary hippocampal neuron culture transfected with myc-GluN2A (D) or myc-GluN2B (E) at 14 or 15 DIV.

Recycling receptor populations are labeled in green, and internalized receptor populations are in red.

(F–I) Histograms represent the means of the ratio of recycled receptor puncta over internalized puncta corresponding, respectively, to the images in (B)–(E). (F) Data were compared using two-way ANOVA (n = 17 to 18 neurons). (G) Data were compared using two-way ANOVA and Bonferroni multiple comparison test (n = 13–15 neurons). (H) Data were compared using two-way ANOVA (n = 15–18 neurons). (I) Data were compared using two-way ANOVA and Bonferroni multiple comparison test (n = 15–20 neurons). Error bars are all ± SEM.

(J and K) Recycling of GluN2A-containing NMDARs with stimulation and overexpression of ARF6-HA, ARF6-DN-HA with GFP-control, or GFP-Scrib1 (J) and histograms represent the means of the ratio of recycled receptor puncta over internalized puncta (K). Data were compared using two-way ANOVA and Bonferroni multiple comparison test (n = 15–20 neurons) ± SEM. Error bars are all ± SEM.

(L and M) Recycling of GluN2A-containing NMDARs with stimulation and overexpression of EFA6-VSVG, EFA6-DN-VSVG with GFP-control, or GFP-Scrib1 (L) and histograms represent the means of the ratio of recycled receptor puncta over internalized puncta (M). Data were compared using two-way ANOVA and Bonferroni multiple comparison test (n = 10) ± SEM. Error bars are all ± SEM.

The scale bar represents 10 μm.
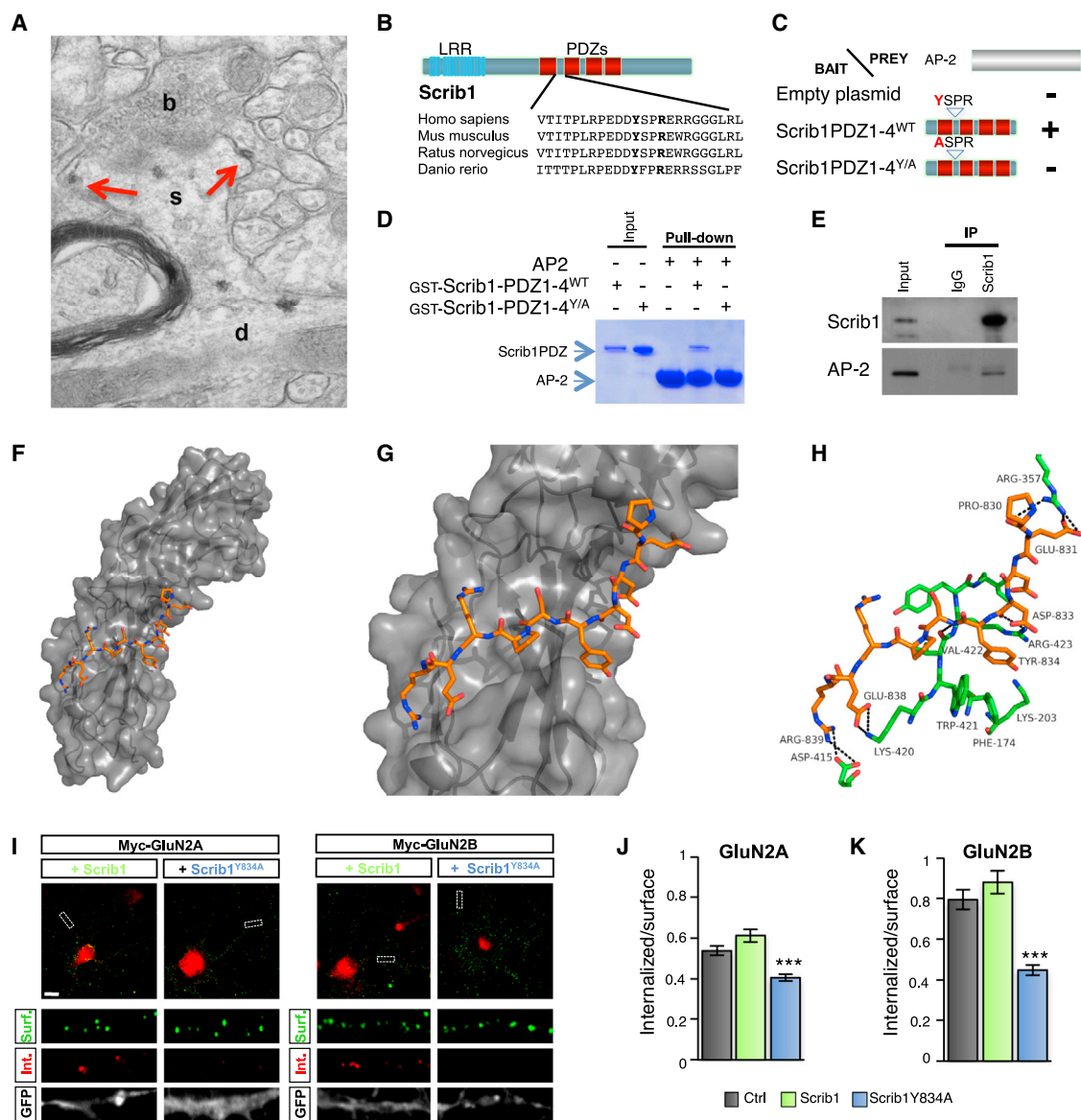
**Figure 6. The Direct Interaction between Scrib1 and AP2 Is Necessary for Internalization of the Scribl1/GluN2 Complex**

(A) Immunolabeling of Scrib1 in a dendritic spine in the CA1 stratum radiatum of the hippocampus. Electron microscopy image shows Scrib1 is found in the PSD and associated with the membrane of the spine (arrows). b, bouton; d, dendrite; s, spine.

(B) Schematic view of the Scrib1 YxxR motif, a conserved AP2 binding motif found between PDZ1 and PDZ2 of Scribble1.

(C) Directed yeast two-hybrid assays with AP2 fragment and Scrib1 PDZ constructs. Schematic of Scrib1 PDZ domain structures used as bait in yeast two-hybrid. Scrib1 binds AP2 via the YxxR binding domain site, and replacement of the lysine (Y) with an alanine (A; AxxR) disrupts this interaction. WT, wild-type.

(D) A pull-down assay indicates that AP2 binds to Scrib1 YxxR His-tagged protein, but not to mutated Scrib1 AxxR.

(E) Coimmunoprecipitation of endogenous Scrib1 and AP2 from the hippocampus. The lysates were immunoprecipitated with Scrib1 antibodies, and the precipitates were immunoblotted for AP2.

(F and G) Overall view of the model of the interaction between the binding region (gray) and the linker between PDZ1 and PDZ2 from Scrib1 (orange). Scrib1 residues 830–839 are represented as sticks, and AP2 is shown as a gray surface model.

(H) Stick model of the interactions of Phe174, Lys203, Arg357, Asp415, and Lys420 to Iso425 (green) with the Pro830 to Arg839 residues from the linker sequence between PDZ1 and PDZ2 from Scrib1 (orange).

(I) Internalization of GluN2A- and GluN2B-containing NMDARs. Myc-GluN2A and GFP-Scrib1 or GFP-Scrib1[Y834A] (left panel) and Myc-GluN2B and GFP-Scrib1 or GFP-Scrib1[Y834A] (right panel) were transfected into 14 or 15 DIV hippocampal neuron culture. The scale bar represents 10 $\mu$m.

(J and K) Histograms represent the means of the ratio of internalized receptor puncta over the surface receptor puncta ± SEM. (J) Data were compared using one-way ANOVA and Bonferroni multiple comparison test (n = 19 to 20 neurons). (K) Data were compared using one-way ANOVA and Bonferroni multiple comparison test (n = 15–18 neurons). Error bars are all ± SEM.
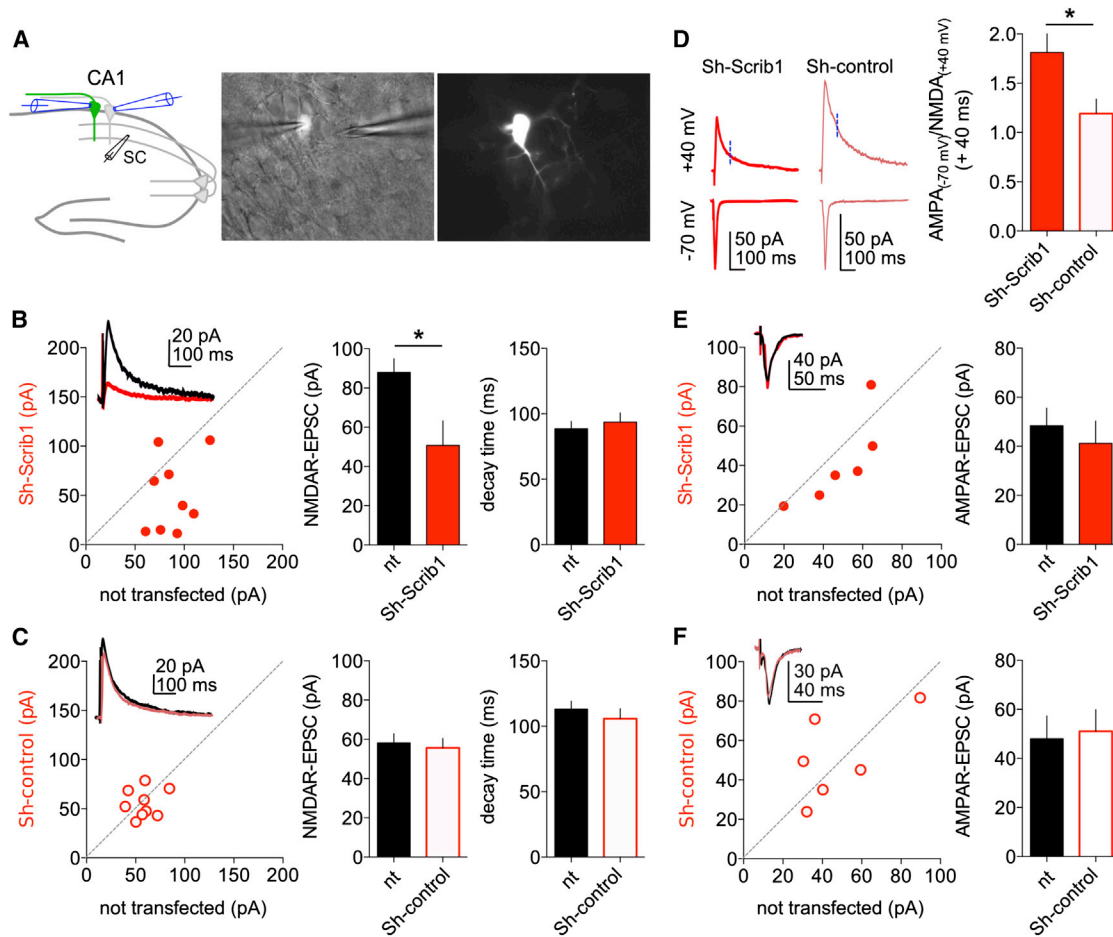
**Figure 7. Scrib1 Regulates the Level of Synaptic NMDARs at Schaffer Collaterals CA1 Pyramidal Cells Synapse**

(A) Schematic cartoon illustrating paired recordings from neighboring electroporated and not electroporated (control) neurons in CA1 pyramidal layer. Whole-cell voltage-clamp recordings were performed at +40 mV while stimulating the Schaffer collaterals (SC) every 10 s. On the right, example images of a pair of recorded neighboring neurons.

(B) Transfection with pSUPER-shRNA-Scrib1 reduces the amplitude of NMDAR-mediates EPSCs at SC-CA1 synapse but does not modify their decay time. Sample traces shown in the inset (control: n = 9; pSUPER-shRNA-Scrib1: n = 9). nt, not transfected.

(C) pSUPER-shRNA-control transfection does not affect the NMDAR-mediates EPSCs at SC-CA1 synapse (amplitude and decay time); sample traces shown in the inset (control: n = 9; pSUPER-shRNA-control: n = 9).

(D) Sample traces and summary graphs illustrating transfection of pSUPER-shRNA-Scrib1 induces a significant change in the AMPA/NMDA ratio when compared to cells transfected with pSUPER-shRNA-control inset (pSUPER-shRNA-Scrib1: n = 10; pSUPER-shRNA-control: n = 11).

(E) Transfection with pSUPER-shRNA-Scrib1 does not modify the amplitude of AMPAR-mediates EPSCs at SC-CA1 synapse (control: n = 6; pSUPER-shRNA-Scrib1: n = 6).

(F) Transfection with pSUPER-shRNA-control does not modify the amplitude of AMPAR-mediates EPSCs at SC-CA1 synapse (control: n = 6; pSUPER-shRNA-control: n = 6).

dissociated hippocampal resulted in a decrease in spine density (Moreau et al., 2010). In the present study, we studied the early effect of Scrib1 loss on NMDAR trafficking, with a reduced post-transfection delay and processing of 48 hr. This shorter time was carefully chosen to minimize spine loss while still having a down-regulation of Scrib1 protein above 70%. The unchanged synaptophysin puncta density after 48 hr posttransfection supports our claim of an absence of massive loss of synapses. Under these experimental conditions, we were able to reveal specific effects of Scrib1 levels on NMDAR trafficking. Our results suggest that the first effect of Scrib1 knockdown in hippocampal

neurons is the decreased levels of GluN2A and GluN2B at the membrane, with a difference in the endocytosis or recycling rates of the two subunits. These differential effects of Scrib1 levels on GluN2A versus GluN2B endocytosis and recycling are consistent with previously observed differences in GluN2A and GluN2B secretory trafficking (Roche et al., 2001; Lavezzari et al., 2004). We showed that this Scrib1-dependent regulation of GluN2A and GluN2B endocytosis and recycling is specific because β3-containing GABA$_A$ receptors are not affected under the same conditions. Moreover, 3 days after transfection of shRNA for Scrib1 in organotypic slice cultures, the loss of Scrib1

in CA1 neurons decreased the amplitude of NMDAR-synaptic currents, but not of AMPAR-EPSCs, supporting the idea that Scrib1 regulates the number of NMDARs present at synapses. The changes in the surface expression of NMDARs could result from either impaired exocytosis of novel receptors or enhanced endocytosis followed by an impaired exocytosis of recycled receptors. Similar effects to Scrib1 on trafficking were also observed for G-protein-coupled receptor thyrotropin receptors (Lahuna et al., 2005) and integrin α5 (Michaelis et al., 2013). This impairment in recycling is presumably due to a failure of the normal recycling pathway in early endosomes that contain GluN2 but lack Scrib1, thus driving the receptors to the late lysosomal compartment. Scrib1 colocalizes strongly with Rab5a and Rab11 in early and recycling endosomes, respectively, suggesting that Scrib1 has a dynamic function in endocytosis and the recycling of NMDARs. Scrib1 is likely to interact with components of the membrane fusion machinery involved in the recycling of NMDARs. Consistent with this, we found that Sec8, a member of the exocyst complex, interacts with Scrib1 in the hippocampus (N.H.P. and N.S., data not shown). It is known that the exocyst complex and ARF6 control postendocytic recycling (Prigent et al., 2003) and that Scrib1 signaling involves ARF6 (Lahuna et al., 2005). Our own data show that ARF6$^{T27N}$ or EFA6$^{E242K}$ constructs both block GluN2A recycling, implicating the ARF6 pathway in the regulation of NMDARs. This is also consistent with previous studies showing that SNAP23 or SNAP25 regulate NMDAR trafficking by acting as a component of the membrane fusion machinery and not by directly binding NMDAR (Lau et al., 2010; Suh et al., 2010). Electron microscopy analysis showed that Scrib1 colocalizes with NMDARs and is often localized to the lateral domain of the spine, where activity-dependent exocytosis and endocytosis domains are present (Kennedy and Ehlers, 2006). Moreover, it has been shown that Scrib1 can form a complex with syntaxin 4 (Massimi et al., 2008), one of the target-membrane-associated SNARE involved in spine exocytosis (Kennedy et al., 2010). We thus favor a model whereby Scrib1 facilitates AP2-dependent internalization of NMDAR and then associates with syntaxin to drive recycling of NMDAR-containing endocytic compartments back to the membrane, probably through a SNARE/exocyst complex.

After the priming of the receptors by D-serine stimulation, the major NMDAR coagonist at the synapse (Papouin et al., 2012), AP2 either binds directly to the NMDARs and drives them to the degradation pathway or binds to Scrib1 and initiates endocytosis and recycling of the NMDAR/Scrib1 complex. Moreover, D-serine stimulation prior to D-serine/NMDA activation affects differently the pool of surface GluN2A and GluN2B. Further work is needed to understand the molecular mechanism underlying the differences upon D-serine stimulation described in this study.

Interestingly, we show that the overexpression of a Scrib1-AP2 binding-defective mutant (Scrib1$^{Y834A}$) reduces both GluN2A and GluN2B internalization (Figure 6J) whereas Scrib1 shRNA has the opposite effect (Figures 5G and 5I). This differential effect of Scrib1 knockdown versus ectopic expression reveals presumably a dominant-negative role of Scrib1$^{Y834A}$. The sh-Scrib1 experiments reveal the effect of the absence of Scrib1 on GluN2A and GluN2B receptors. Indeed, we showed that GluN2A endocytosis increases in absence of Scrib1 expression.

We believe this emphasizes the role of Scrib1 on the stabilization of GluN2A at the membrane. Hence, in absence of Scrib1, GluN2A is less stable, and nothing prevents the direct binding of AP2 to the subunit and its internalization (Lavezzari et al., 2004). On the contrary, GluN2B endocytosis decreases in absence of Scrib1 expression, supporting an active role for Scrib1 in the endocytosis process, but not in the stabilization of the GluN2B subunit. In presence of Scrib1$^{Y834A}$ mutant, both GluN2A and GluN2B endocytosis is reduced, revealing the dependence of each subunit on the AP2 binding motif of Scrib1 for endocytosis. Here, the mutated Scrib1 can still bind the subunits via the PDZ domains and fulfil some of its function: stabilization for GluN2A and blocking of the internalization for GluN2B. However, the mutation of the AP2 motif on Scrib1$^{Y834A}$ partially affects some of Scrib1 downstream effects, revealing an AP2-dependent mechanism in NMDAR-induced internalization via Scrib1. Only one previous study has described a direct interaction between a cytoplasmic cargo protein and the μ-adaptin subunits during membrane receptor internalization. In Yu et al. (2007), the authors showed that the planar cell polarity protein Dishevelled associates with AP2 to induce the endocytosis of Frizzled coupled to its degradation (Yu et al., 2007). Interestingly, Scrib1, which is also a planar cell polarity protein, couples the internalization of the receptors to recycling.

We found that the interaction between GluN2 and Scrib1 is mediated by the carboxy-terminal PDZ-BD of GluN2 and the Scrib1 PDZ domains 2 and 3 because a Scrib1 form lacking these two domains has no influence on NMDAR trafficking. NMDARs have been shown to bind numerous PDZ proteins, including all four members of the PSD-95 family of MAGUKs (PSD-95, SAP102, PSD-93, and SAP97), MAGI1–MAGI3, MALS1–MALS3, CIPP, and GIPC (Wenthold et al., 2003; Yi et al., 2007); several of these proteins play roles in anchoring the receptors (Roche et al., 2001; Sans et al., 2000) and likely compete with Scrib1 for NMDAR binding. Various studies have shown that AP2 binds directly to NMDARs (Prybylowski et al., 2005; Scott et al., 2004) and that, after direct binding to AP2, GluN2A or GluN2B are degraded, except when AP2 binds the YEKL motif near the PDZ-BD of GluN2B (Scott et al., 2004). We and others have shown that Fyn kinase or hippocalcin can cause the dissociation of PSD-95 from NMDARs, allowing AP2 to bind to the receptors, thus inducing their internalization (Jo et al., 2010; Prybylowski et al., 2005). Our model shows that Scrib1 can stabilize GluN2A-containing NMDARs in basal conditions, whereas upon activation, Scrib1 leads to the entry of GluN2A-containing NMDARs into the recycling pathway. In contrast, Scrib1 plays a role in GluN2B-containing NMDAR trafficking by preventing their recycling upon stimulation. These different mechanisms maintain the GluN2A/GluN2B ratio in basal conditions and mediate the switch from surface GluN2B to GluN2A, leading to an increased GluN2A/GluN2B ratio upon stimulation. The fact that GluN2A can be recycled in the presence of Scrib1 after the activation of NMDARs is consistent with the concept that the activation pathways of distinct NMDARs use different scaffold and adaptor complexes for proper intracellular traffic and regulation. It is also possible that Scrib1 participates in the direct sorting of NMDAR. Our data using a mutated form of Scrib1 missing the two PDZ domains seem to argue against

the latter hypothesis (Figures 3A–3F), but additional experiments will be needed to answer this question.

We showed that, in the presence of Scrib1, GluN2A can recycle back to the membrane, and thus GluN2B is not the only NMDAR subunit that can recycle. This dual mechanism has been known for a long time for AMPARs. It has been demonstrated quite convincingly that activation of NMDAR triggers internalization and recycling of GluA1-containing AMPARs and that GluA2 and GluA2/GluA3 constitutively recycle (Barry and Ziff, 2002; Ehlers, 2000; Henley et al., 2011; Shepherd and Huganir, 2007). It will be important for future studies to assess the specific consequences of the recycling of GluN2A on AMPAR trafficking at synapses.

Together, our results show that Scrib1 is a key scaffolding molecule regulated by activity in vivo and in vitro and that it is responsible for the internalization and recycling of NMDA receptors. Together with recent publications (Groc et al., 2006; Prybylowski et al., 2005; Suh et al., 2010), our work strengthens the emerging idea that different PDZ proteins regulate GluR trafficking at the membrane via the endosomal system. This mechanism involving Scrib1 is likely to be implicated in the regulation of synapse function in numerous physiological processes and pathological states that involve interactions between NMDARs, Scrib1, and AP2.

## EXPERIMENTAL PROCEDURES

### Animals
All rats were Sprague-Dawley between embryonic day 18 (E18) and 10 weeks old at the time of experiments. Rats had free access to food and water and were housed in polypropylene cages under controlled conditions (at $23°C \pm 1°C$, with lights on from 7:00 a.m. to 7:00 p.m,, assuring a 12:12 hr light/dark cycle), with the behavioral testing or the other experiments performed during the light portion of the cycle. All procedures were performed according to the requirements of the United Kingdom Animals (Scientific Procedures) Act 1986, AWERB Newcastle University (ID: 374), the European Communities Council Directives (86/609/EEC), and the French National Committee (87/848) recommendations.

### Antibodies and Vector Constructions
The detailed information on antibodies and constructs used in this study are in the Supplemental Experimental Procedures.

### Yeast Two-Hybrid Assays
pGBKT7-GluN2A and pGBKT7-GluN2B were used as described previously (Yi et al., 2007). Scrib1[PDZ] (amino acids 712–1,187 of the Q80U72-3 sequence) was subcloned into pGAD and pGBTK7 and modified by site-directed mutagenesis (Stratagen). Yeast two-hybrid screening was performed only once with the library, and yeast assays to confirm the interaction were performed at least three times as described in the Clontech protocol.

### Detergent Solubilization and Immunoprecipitation Experiment
IP experiments were performed after 1% sodium deoxycholate, 0.1% Triton X-100 solubilization as described previously (Sans et al., 2003).

### Culture and Transfections of Hippocampal Neurons
Primary hippocampal cultures were prepared from E18 Sprague-Dawley rats. Cultures were transfected with the different constructs at 12 or 14 days in culture using the calcium phosphate method (Moreau et al., 2010; Sans et al., 2005).

### Surface, Internalization, and Recycling Experiments in Neurons
Hippocampal neurons (12 days in vitro [DIV]) were transfected with GFP control or GFP-Scrib1; control shRNA or Scrib1 shRNA; or myc-tagged GluN2A,

GluN2B, or $GABA_A$ $\beta3$ using calcium phosphate methods (Sans et al., 2003). The experiments were performed 36–48 hr after transfection. The protocol to measure recycled NMDARs after internalization in hippocampal neurons was adapted from previous studies (Suh et al., 2010). The stimulation was adapted from Nong et al. (2003). Briefly, prestimulation with D-serine (100 μM) was performed for 5 min followed by a stimulation with NMDA (50 μM) plus D-serine (1 μM) over 5 min before the internalization step. See also the Supplemental Experimental Procedures.

### Data Presentation and Statistical Analysis
The results are described as mean ± SEM or whiskers boxes. Two-way ANOVA, one-way ANOVA, or Kruskal-Wallis one way was performed where indicated. For most experiments, the Student's t test was used to determine statistical significance (*p < 0.05; **p < 0.01; ***p < 0.001). Statistical analyses were performed using the Statistica or GraphPad Prism statistical package (GraphPad). See also the Supplemental Experimental Procedures and Table S2.

### Additional Methods
Details regarding the methods used for ITC, pull-down assays; fractionation; culture and transfections of HEK293 or COS-7 cells; surface, internalization, and recycling experiments in fibroblasts and neurons; pre-embedding immunocytochemistry or postembedding immunogold; electrophysiological recordings in slice; and data analysis are provided in the Supplemental Experimental Procedures.

## SUPPLEMENTAL INFORMATION

Supplemental Information includes Supplemental Experimental Procedures, seven figures, and two tables and can be found with this article online at http://dx.doi.org/10.1016/j.celrep.2014.09.017.

## REFERENCES

Barria, A., and Malinow, R. (2002). Subunit-specific NMDA receptor trafficking to synapses. Neuron 35, 345–353.

Barry, M.F., and Ziff, E.B. (2002). Receptor trafficking and the plasticity of excitatory synapses. Curr. Opin. Neurobiol. *12*, 279–286.

Chung, H.J., Huang, Y.H., Lau, L.F., and Huganir, R.L. (2004). Regulation of the NMDA receptor complex and trafficking by activity-dependent phosphorylation of the NR2B subunit PDZ ligand. J. Neurosci. *24*, 10248–10259.

Ehlers, M.D. (2000). Reinsertion or degradation of AMPA receptors determined by activity-dependent endocytic sorting. Neuron *28*, 511–525.

Elias, G.M., and Nicoll, R.A. (2007). Synaptic trafficking of glutamate receptors by MAGUK scaffolding proteins. Trends Cell Biol. *17*, 343–352.

Follows, E.R., McPheat, J.C., Minshull, C., Moore, N.C., Pauptit, R.A., Rowsell, S., Stacey, C.L., Stanway, J.J., Taylor, I.W., and Abbott, W.M. (2001). Study of the interaction of the medium chain mu 2 subunit of the clathrin-associated adapter protein complex 2 with cytotoxic T-lymphocyte antigen 4 and CD28. Biochem. J. *359*, 427–434.

Franco, M., Peters, P.J., Boretto, J., van Donselaar, E., Neri, A., D'Souza-Schorey, C., and Chavrier, P. (1999). EFA6, a sec7 domain-containing exchange factor for ARF6, coordinates membrane recycling and actin cytoskeleton organization. EMBO J. *18*, 1480–1491.

Groc, L., Heine, M., Cousins, S.L., Stephenson, F.A., Lounis, B., Cognet, L., and Choquet, D. (2006). NMDA receptor surface mobility depends on NR2A-2B subunits. Proc. Natl. Acad. Sci. USA *103*, 18769–18774.

Groc, L., Bard, L., and Choquet, D. (2009). Surface trafficking of N-methyl-D-aspartate receptors: physiological and pathological perspectives. Neuroscience *158*, 4–18.

Henley, J.M., Barker, E.A., and Glebov, O.O. (2011). Routes, destinations and delays: recent advances in AMPA receptor trafficking. Trends Neurosci. *34*, 258–268.

Howard, M.A., Elias, G.M., Elias, L.A., Swat, W., and Nicoll, R.A. (2010). The role of SAP97 in synaptic glutamate receptor dynamics. Proc. Natl. Acad. Sci. USA *107*, 3805–3810.

Jo, J., Son, G.H., Winters, B.L., Kim, M.J., Whitcomb, D.J., Dickinson, B.A., Lee, Y.B., Futai, K., Amici, M., Sheng, M., et al. (2010). Muscarinic receptors induce LTD of NMDAR EPSCs via a mechanism involving hippocalcin, AP2 and PSD-95. Nat. Neurosci. *13*, 1216–1224.

Jurd, R., Thornton, C., Wang, J., Luong, K., Phamluong, K., Kharazia, V., Gibb, S.L., and Ron, D. (2008). Mind bomb-2 is an E3 ligase that ubiquitinates the N-methyl-D-aspartate receptor NR2B subunit in a phosphorylation-dependent manner. J. Biol. Chem. *283*, 301–310.

Kennedy, M.J., and Ehlers, M.D. (2006). Organelles and trafficking machinery for postsynaptic plasticity. Annu. Rev. Neurosci. *29*, 325–362.

Kennedy, M.J., Davison, I.G., Robinson, C.G., and Ehlers, M.D. (2010). Syntaxin-4 defines a domain for activity-dependent exocytosis in dendritic spines. Cell *141*, 524–535.

Lahuna, O., Quellari, M., Achard, C., Nola, S., Méduri, G., Navarro, C., Vitale, N., Borg, J.P., and Misrahi, M. (2005). Thyrotropin receptor trafficking relies on the hScrib-betaPIX-GIT1-ARF6 pathway. EMBO J. *24*, 1364–1374.

Lau, C.G., and Zukin, R.S. (2007). NMDA receptor trafficking in synaptic plasticity and neuropsychiatric disorders. Nat. Rev. Neurosci. *8*, 413–426.

Lau, C.G., Takayasu, Y., Rodenas-Ruano, A., Paternain, A.V., Lerma, J., Bennett, M.V., and Zukin, R.S. (2010). SNAP-25 is a target of protein kinase C phosphorylation critical to NMDA receptor trafficking. J. Neurosci. *30*, 242–254.

Lavezzari, G., McCallum, J., Dewey, C.M., and Roche, K.W. (2004). Subunit-specific regulation of NMDA receptor endocytosis. J. Neurosci. *24*, 6383–6391.

Losi, G., Prybylowski, K., Fu, Z., Luo, J., Wenthold, R.J., and Vicini, S. (2003). PSD-95 regulates NMDA receptors in developing cerebellar granule neurons of the rat. J. Physiol. *548*, 21–29.

Massimi, P., Narayan, N., Thomas, M., Gammoh, N., Strand, S., Strand, D., and Banks, L. (2008). Regulation of the hDlg/hScrib/Hugl-1 tumour suppressor complex. Exp. Cell Res. *314*, 3306–3317.

Mauceri, D., Gardoni, F., Marcello, E., and Di Luca, M. (2007). Dual role of CaMKII-dependent SAP97 phosphorylation in mediating trafficking and insertion of NMDA receptor subunit NR2A. J. Neurochem. *100*, 1032–1046.

Michaelis, U.R., Chavakis, E., Kruse, C., Jungblut, B., Kaluza, D., Wandzioch, K., Manavski, Y., Heide, H., Santoni, M.J., Potente, M., et al. (2013). The polarity protein Scrib is essential for directed endothelial cell migration. Circ. Res. *112*, 924–934.

Montgomery, J.M., Selcher, J.C., Hanson, J.E., and Madison, D.V. (2005). Dynamin-dependent NMDAR endocytosis during LTD and its dependence on synaptic state. BMC Neurosci. *6*, 48.

Moreau, M.M., Piguel, N., Papouin, T., Koehl, M., Durand, C.M., Rubio, M.E., Loll, F., Richard, E.M., Mazzocco, C., Racca, C., et al. (2010). The planar polarity protein Scribble1 is essential for neuronal plasticity and brain function. J. Neurosci. *30*, 9738–9752.

Nong, Y., Huang, Y.Q., Ju, W., Kalia, L.V., Ahmadian, G., Wang, Y.T., and Salter, M.W. (2003). Glycine binding primes NMDA receptor internalization. Nature *422*, 302–307.

Papouin, T., Ladépêche, L., Ruel, J., Sacchi, S., Labasque, M., Hanini, M., Groc, L., Pollegioni, L., Mothet, J.P., and Oliet, S.H. (2012). Synaptic and extrasynaptic NMDA receptors are gated by different endogenous coagonists. Cell *150*, 633–646.

Pérez-Otaño, I., Luján, R., Tavalin, S.J., Plomann, M., Modregger, J., Liu, X.B., Jones, E.G., Heinemann, S.F., Lo, D.C., and Ehlers, M.D. (2006). Endocytosis and synaptic removal of NR3A-containing NMDA receptors by PACSIN1/syndapin1. Nat. Neurosci. *9*, 611–621.

Prigent, M., Dubois, T., Raposo, G., Derrien, V., Tenza, D., Rossé, C., Camonis, J., and Chavrier, P. (2003). ARF6 controls post-endocytic recycling through its downstream exocyst complex effector. J. Cell Biol. *163*, 1111–1121.

Prybylowski, K., Chang, K., Sans, N., Kan, L., Vicini, S., and Wenthold, R.J. (2005). The synaptic localization of NR2B-containing NMDA receptors is controlled by interactions with PDZ proteins and AP-2. Neuron *47*, 845–857.

Roche, K.W., Standley, S., McCallum, J., Dune Ly, C., Ehlers, M.D., and Wenthold, R.J. (2001). Molecular determinants of NMDA receptor internalization. Nat. Neurosci. *4*, 794–802.

Sans, N., Petralia, R.S., Wang, Y.X., Blahos, J., 2nd, Hell, J.W., and Wenthold, R.J. (2000). A developmental change in NMDA receptor-associated proteins at hippocampal synapses. J. Neurosci. *20*, 1260–1271.

Sans, N., Prybylowski, K., Petralia, R.S., Chang, K., Wang, Y.X., Racca, C., Vicini, S., and Wenthold, R.J. (2003). NMDA receptor trafficking through an interaction between PDZ proteins and the exocyst complex. Nat. Cell Biol. *5*, 520–530.

Sans, N., Wang, P.Y., Du, Q., Petralia, R.S., Wang, Y.X., Nakka, S., Blumer, J.B., Macara, I.G., and Wenthold, R.J. (2005). mPins modulates PSD-95 and SAP102 trafficking and influences NMDA receptor surface expression. Nat. Cell Biol. *7*, 1179–1190.

Sanz-Clemente, A., Matta, J.A., Isaac, J.T., and Roche, K.W. (2010). Casein kinase 2 regulates the NR2 subunit composition of synaptic NMDA receptors. Neuron *67*, 984–996.

Sanz-Clemente, A., Gray, J.A., Ogilvie, K.A., Nicoll, R.A., and Roche, K.W. (2013). Activated CaMKII couples GluN2B and casein kinase 2 to control synaptic NMDA receptors. Cell Reports *3*, 607–614.

Scott, D.B., Michailidis, I., Mu, Y., Logothetis, D., and Ehlers, M.D. (2004). Endocytosis and degradative sorting of NMDA receptors by conserved membrane-proximal signals. J. Neurosci. *24*, 7096–7109.

Sheng, M., and Hoogenraad, C.C. (2007). The postsynaptic architecture of excitatory synapses: a more quantitative view. Annu. Rev. Biochem. *76*, 823–847.

Shepherd, J.D., and Huganir, R.L. (2007). The cell biology of synaptic plasticity: AMPA receptor trafficking. Annu. Rev. Cell Dev. Biol. *23*, 613–643.

Suh, Y.H., Terashima, A., Petralia, R.S., Wenthold, R.J., Isaac, J.T., Roche, K.W., and Roche, P.A. (2010). A neuronal role for SNAP-23 in postsynaptic glutamate receptor trafficking. Nat. Neurosci. *13*, 338–343.

Traub, L.M. (2009). Tickets to ride: selecting cargo for clathrin-regulated internalization. Nat. Rev. Mol. Cell Biol. *10*, 583–596.

Traynelis, S.F., Wollmuth, L.P., McBain, C.J., Menniti, F.S., Vance, K.M., Ogden, K.K., Hansen, K.B., Yuan, H., Myers, S.J., and Dingledine, R. (2010). Glutamate receptor ion channels: structure, regulation, and function. Pharmacol. Rev. *62*, 405–496.

Uekita, T., Itoh, Y., Yana, I., Ohno, H., and Seiki, M. (2001). Cytoplasmic tail-dependent internalization of membrane-type 1 matrix metalloproteinase is important for its invasion-promoting activity. J. Cell Biol. *155*, 1345–1356.

Wenthold, R.J., Prybylowski, K., Standley, S., Sans, N., and Petralia, R.S. (2003). Trafficking of NMDA receptors. Annu. Rev. Pharmacol. Toxicol. *43*, 335–358.

Yashiro, K., and Philpot, B.D. (2008). Regulation of NMDA receptor subunit expression and its implications for LTD, LTP, and metaplasticity. Neuropharmacology *55*, 1081–1094.

Yi, Z., Petralia, R.S., Fu, Z., Swanwick, C.C., Wang, Y.X., Prybylowski, K., Sans, N., Vicini, S., and Wenthold, R.J. (2007). The role of the PDZ protein GIPC in regulating NMDA receptor trafficking. J. Neurosci. *27*, 11663–11675.

Yu, A., Rual, J.F., Tamai, K., Harada, Y., Vidal, M., He, X., and Kirchhausen, T. (2007). Association of Dishevelled with the clathrin AP-2 adaptor is required for Frizzled endocytosis and planar cell polarity signaling. Dev. Cell *12*, 129–141.